Experimental Assessment of Point Kernel Shielding Calculation Codes : QAD and G33

T. Miura[1], N. Odano[1], Y. Shindo[2]

[1]Ship Research Institute, Tokai Branch, Ibaraki-ken, Japan
[2]Mitsubishi Research Institute Inc. Tokyo, Japan

INTRODUCTION

Japan is scheduled to transport a large amount of radioactive wastes by exclusive vessels mainly from domestic nuclear plants to the low level radioactive waste storage facility starting in fiscal 1992. To establish radiation safety in the transportation, it is necessary to keep the radiation exposure of transport workers and the general public as low as reasonably achievable. Although radiation levels of these wastes are mostly low, wastes of some percentage contain radioactive materials of too high levels to carry them without shielding. To carry these wastes, steel containers having an appropriate wall thickness can be used, each of which probably contains several drums packed with radioactive wastes. To design such a container, point kernel calculation codes will be used. These codes also have been used to calculate the performance of shields to be installed in exclusive vessels. Since the accuracy of point kernel calculations varies depending on the problem, it is necessary to assess these codes for shielding problems to be appeared in the low level radioactive wastes transportation. In this study, applicability of point kernel calculations to the design of steel containers was investigated. Furthermore, the accuracy of these calculations was examined regarding problems of the reflection and the slant penetration.

EXPERIMENT

Three experiments were carried out using ^{60}Co and ^{137}Cs isotopes as gamma-ray sources. Structure of the ^{60}Co source is shown in Fig. 1. Cobalt wires of 4.7 cm long and 0.1 cm diameter were formed into cylindrical shape. A stick-type ^{137}Cs source contained in a 5-cm-long and 2-cm-diameter cylindrical aluminum case was used. Through the experiments, intensities of these sources were normalized to 1.59×10^{10} Bq for the ^{60}Co source and 1.81×10^{10} Bq for the ^{137}Cs source, respectively. Exposure rates were measured by

thermoluminescent dosimeters (TLDs) which were type UD-200S produced by Matsushita Electric Co. Ltd. Structure of the UD-200S dosimeter is shown in Fig. 2. Two glass capsules containing $CaSO_4$(Tm) powder are covered with shielding caps made of an alloy. Energy responses of UD-200S TLDs were measured by irradiating them in the field of which intensities were determined by using a calibrated ionization chamber within an accuracy of ±3%. The response measurements were carried out at energies of 1.25, 0.661, 0.177 and 0.0492 MeV, respectively. The result is shown in Fig. 3. The detector response for gamma rays is approximately flat above about 30 keV. Responses at 1.25 and 0.661 MeV were used as conversion factors of readings to exposures in the ^{60}Co experiments and in the ^{137}Cs experiment, respectively. These factors were determined within an accuracy of ±4.1% at 1.25 MeV, and ±5.7% at 0.661 MeV. Readings of the UD-200S TLD vary widely and about 10% was considered as the amount of scatter in readings.

In the first experiment, four concrete cylinders, which simulate drums packed with cemented radioactive wastes, were set in a steel box which was placed on a steel rack of 1 m in height. Dimensions of the concrete cylinders are 60 cm in diameter and 90 cm in height. The steel box has an inside dimension of 135 x 135 x 100 cm and a wall thickness of 3.2 cm. The ^{60}Co source was set at the center of one of the concrete cylinders. The experimental arrangement is shown in Fig. 4 together with measurement positions and numbers. Measurement numbers in Fig. 4 were designated in XY planes of Z=48.2, 88.2, 107.0 and 206.4 cm in the same way.

The second experiment is on the reflection. The ^{60}Co or the ^{137}Cs source was placed at a position of 50 cm away from a 1-meter-square concrete plate of 20 cm thick and exposure rates of gamma rays reflected from the concrete plate were measured at five positions as shown in Fig. 5. A lead block was placed between the source and the detectors to eliminate the direct gamma rays from the source to the detectors. To estimate room scattering, gamma rays were also measured in an arrangement without the concrete plate. Exposure rates of the reflected gamma rays were obtained from the differences of those measured with and without the concrete plate. The third experiment is on the slant penetration. The ^{60}Co source was placed on one side of a concrete plate of which the dimension is 1m x 2m x 20 cm. Thermoluminescent dosimeters were placed along the other side of the concrete plate. A layout of the experiment is shown in Fig. 6.

Atomic densities of ordinary concretes used in the first experiment and in the second and third experiments are given in Table 1, respectively. They were measured by a chemical analysis. The analysis was carried out when weights of concrete test pieces became stable. Measured densities of

the concretes are 2.15 and 2.23 g/cm^3, respectively.

CALCULATION

Point kernel calculations were carried out by using the QAD-CGGP2 and G33-CGGP2 codes (Sakamoto and Tanaka, 1990), the revised versions of the QAD-CGGP and G33-CGGP codes. Concrete buildup factors were used in these calculations. For the analysis of the second and third experiments, the MCNP Monte Carlo code (Briesmeister, 1986) was also used. For the first experiment, calculations were carried out by the QAD and G33 codes. In the case of the G33 code, the single scattering components from the three concrete blocks and the six iron walls was calculated. The scattering component from the source block was not included in this calculation. The result was added to "the direct beam with buildup factor." Analysis of the reflection experiment and the slant penetration was carried out by the G33 code and the MCNP code. In the case of the reflection analysis, the lead block was taken into consideration. In the G33 calculations, the effect of the spatial mesh interval taken in the concrete plate was examined by changing mesh sizes. However, variation of less than 2% was found in results. In the analysis of the slant penetration, the single scattering component was calculated by taking fine spatial meshes in the thin regions of both sides of the concrete plate, that is, 0.1 cm interval to the Z direction in the 1-cm-thick regions from the both surfaces.

COMPARISON OF MEASUREMENTS AND CALCULATIONS

Comparison of calculations and measurements for the first experiment is given in Table 2. Calculations by the QAD code with concrete buildup factors show a fairly good agreement or overestimation in the vicinity of the source block, outside of the nearest steel wall to the source, and above the upper wall of the container where exposure rates are large and reliable estimation is necessary from the standpoint of the shielding design of the container. Rather large overestimations of more than a factor of 2 are found in the some positions in XY planes of Z=107 and 206.4 cm. One reason for the overestimations is the usage of buildup factors for a point source in finite media. Underestimations are found in the shadow region behind the adjacent two concrete blocks with respect to the source block where scattered gamma rays should be taken into account. Contributions of the single scattering components from the iron walls and the concrete blocks are included in the G33 values in Table 2. In the table, ratios of the single scattering components to total exposure rates are also given in percentage, enclosed in the parentheses. Addition of the single scattering components to total exposure rates improved results; however, this improvement is not satisfactory. As described below,

multiple scattering is necessary to consider in the reflection problem; however, this is beyond point kernel calculations.

Ratios of calculated and measured exposure rates of the second experiment are given in Table 3. Large underestimation is seen in the result of the G33 code. A fairly good agreement is found between Monte Carlo calculations and measurements. Monte Carlo calculations indicated that scattering of about five times per one incident photon occurred in the concrete plate. Therefore, neglecting multiple scattering in the G33 code resulted in the underestimation in the reflection calculation. Underestimation appearing in the shadow region of the first experiment is probably due to the same reason. Values of C/E of the slant penetration are given in Table 4 together with Monte Carlo calculations. In the case of the G33 code, "the direct beam with buildup factor" agreed well with measurements except the measurement positions at Y=80, 90 and 100 cm where gamma rays scattered in the thin regions close to the shield surfaces play important role. "The direct beam without buildup factor" plus the single scattering component calculated with fine spatial meshes in these regions gave a better result. However, not only this calculation but Monte Carlo calculations underestimate when the slant angle becomes large.

CONCLUSIONS

(1) QAD and G33 calculations give values in safer side where the scattering component is not dominant. These codes can be utilized in the design of radioactive waste containers.
(2) Large underestimations were found in the shadow region of cylindrical concrete blocks in an iron box. Point kernel calculation codes is not reliable in such a region.
(3) Multiple scattering cannot be neglected in the reflection problem. Therefore, large underestimation is expected in the calculations by the G33 code.
(4) For the slant penetration, "the direct beam with buildup factor" underestimates exposure rates in the region where the slant angle is large. In the case of the G33 code, it is recommended to take fine spatial meshes in the thin regions close to the surfaces of the shield.
(5) MCNP calculations give satisfactory results in the problem of the reflection. Underestimations were found in the slant penetration problem. Further investigation is necessary to clarify the reason of underestimations.

REFERENCES

J. Briesmeister (Editor), LA-7396-M, Rev. 2 (1986)
Y. Sakamoto and S. Tanaka, JAERI-M 90-110 (1990)

Table 1. Atomic Densities of Concrete Used in the First, Second, and Third Experiments

Element	Atom Density (cm^{-3}) (A) *	(B)
H	1.16+22	1.20+22
O	4.10+22	4.25+22
Si	1.34+22	1.38+21
Al	2.64+21	2.74+21
Fe	5.56+20	5.29+20
Ca	2.58+21	2.58+21
Mg	3.73+20	3.87+20
S	8.08+19	1.26+20
Na	6.76+20	8.77+20
K	4.97+20	6.19+20

* Read as 1.16x10 22

(A) for the first experiment.
(B) for the second and the third experiments.

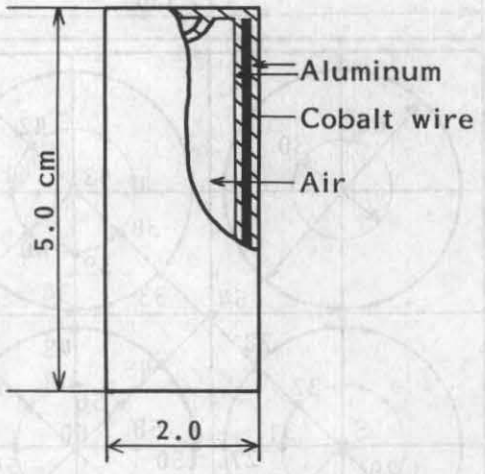

Fig. 1. Structure of the ^{60}Co source.

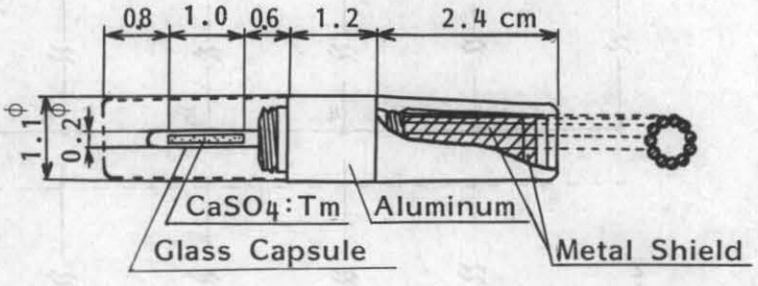

Fig. 2. Structure of the UD-200S TLD.

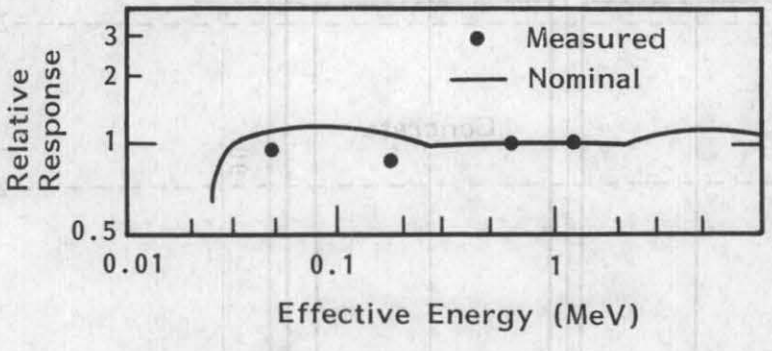

Fig. 3. Relative response of the UD-200S TLD.

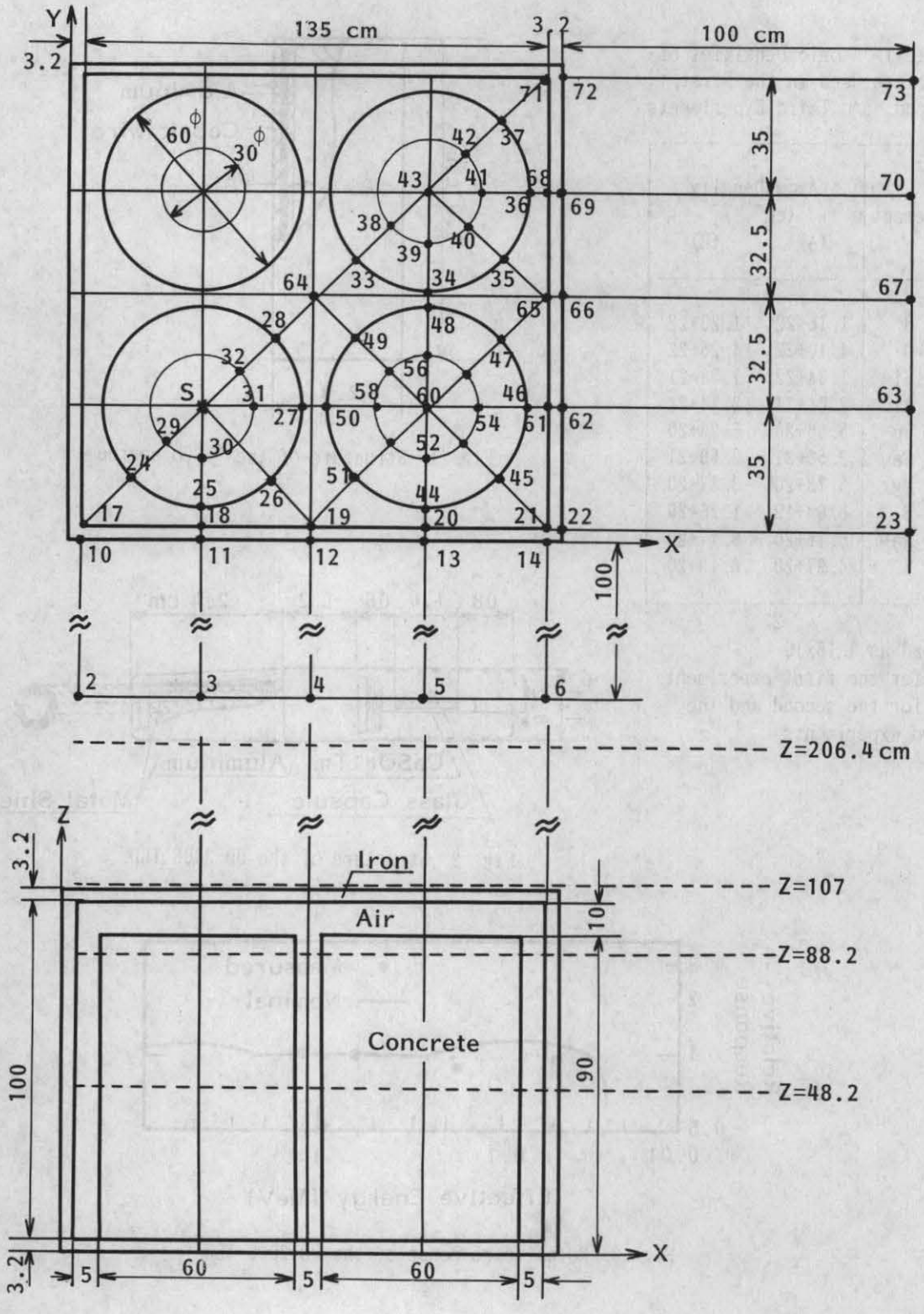

Fig. 4. The arrangement and mesurement positions of the first experiment.

Table 2. Ratios of Calculated and Measured Exposure Rates

No.	Z=48.2cm G33(Rs)	QAD	Z=88.2cm G33(Rs)	QAD	Z=107cm G33(Rs)	QAD	Z=206.4cm G33(Rs)	QAD
2	1.52(13)	1.54	-	-	1.50(14)	1.52	1.06(24)	0.89
4	1.52(13)	1.54	-	-	1.45(15)	1.46	1.01(26)	0.83
6	1.64(15)	1.62	-	-	1.70(15)	1.68	1.41(23)	1.25
10	1.34(8)	1.44	1.48(12)	1.50	-	-	2.13(8)	2.19
11	1.39(9)	1.47	1.62(16)	1.51	-	-	2.07(9)	2.10
12	1.49(12)	1.53	1.69(18)	1.58	-	-	1.97(9)	2.00
13	1.81(22)	1.65	2.08(32)	1.61	-	-	-	-
14	0.80(34)	0.56	0.51(35)	0.33	-	-	1.12(18)	1.04
18	1.10(1)	1.25	1.27(3)	1.17	1.32(1)	1.50	-	-
20	1.77(5)	1.93	1.77(5)	1.88	2.41(22)	2.14	-	-
21	0.69(29)	0.49	0.52(32)	0.35	-	-	-	-
22	1.33(30)	0.93	0.98(33)	0.66	-	-	1.26(17)	1.19
23	0.52(53)	0.24	-	-	0.34(57)	0.15	0.60(40)	0.38
24	1.37(1)	1.36	1.17(3)	1.21	1.85(11)	1.63	-	-
27	1.11(1)	1.26	1.20(3)	1.09	1.66(13)	1.62	-	-
28	1.21(1)	1.37	1.33(2)	1.21	1.81(12)	1.79	-	-
31	-	-	-	-	1.55(8)	1.59	-	-
32	-	-	-	-	1.71(14)	1.65	-	-
34	1.52(4)	1.67	1.57(4)	1.70	2.02(30)	1.61	-	-
35	1.32(27)	1.01	0.96(28)	0.73	-	-	-	-
36	1.83(32)	1.24	1.27(36)	0.81	-	-	-	-
37	1.99(36)	1.29	0.90(44)	0.51	1.75(41)	1.08	-	-
38	-	-	-	-	3.20(61)	1.40	-	-
39	-	-	-	-	1.77(16)	1.70	-	-
42	-	-	-	-	2.31(43)	1.38	-	-
43	-	-	-	-	2.84(50)	1.59	-	-
44	0.78(24)	0.66	0.61(27)	0.46	-	-	-	-
45	0.79(41)	0.46	0.57(48)	0.29	-	-	-	-
46	1.37(36)	0.88	0.56(40)	0.34	-	-	-	-
47	0.58(47)	0.30	0.36(57)	0.15	-	-	-	-
48	0.87(19)	0.70	0.61(23)	0.47	1.86(41)	1.19	-	-
54	-	-	-	-	1.85(28)	1.33	-	-
56	-	-	-	-	1.61(23)	1.29	-	-
58	-	-	-	-	1.69(14)	1.65	-	-
60	-	-	-	-	2.14(29)	1.57	-	-
61	1.01(38)	0.62	0.52(44)	0.29	0.96(37)	0.61	-	-
62	1.60(38)	0.99	0.86(43)	0.49	-	-	-	-
64	-	-	-	-	1.52(10)	1.37	2.03(10)	1.89
65	0.55(49)	0.28	0.40(56)	0.18	0.57(66)	0.20	-	-
66	0.85(53)	0.40	0.62(60)	0.25	-	-	1.13(21)	1.01
67	0.58(71)	0.17	-	-	0.46(75)	0.12	0.66(67)	0.36
68	2.08(30)	1.45	1.21(34)	0.79	1.86(27)	1.36	-	-
69	2.10(31)	1.43	1.54(36)	0.98	-	-	-	-
71	1.80(38)	1.11	0.62(54)	0.28	-	-	-	-
72	1.39(38)	0.85	0.61(56)	0.27	-	-	1.87(4)	1.67
73	2.43(13)	2.11	-	-	2.31(13)	2.01	0.93(28)	0.70

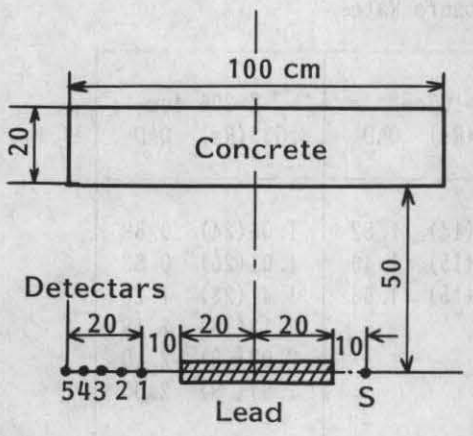

Fig. 5. A layout of the reflection experiment.

Table 3. Comparison of Measured and Calculated Exposure Rates Due to Gamma Rays Reflected from a Concrete Plate

Detector Position	Co-60			Cs-137	
	Measured (mR/h)	C/E (G33)	C/E (MCNP)	Measured (mR/h)	C/E (G33)
1	10.1	0.503	0.811	12.1	0.539
2	8.70	0.571	0.888	11.5	0.537
3	7.87	0.611	0.921	10.6	0.559
4	7.46	0.623	0.913	9.76	0.576
5	7.02	0.634	0.917	8.88	0.601

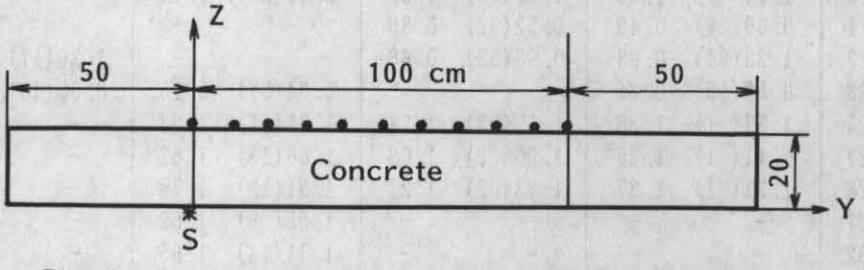

Fig. 6. A layout of the slant penetration experiment.

Table 4. Comparison of Calculated and Measured Exposure Rates Due to Gamma Rays Penetrated Through a Concrete Plate

Y (cm)	Measured (mR/h)	MCNP (mR/h)	C/E	(a) G33 case 1 (mR/h)	C/E	(b) G33 case 2 (mR/h)	C/E
0	1.48+3 *	1.81+3	1.22	1.47+3	0.99	1.21+3	0.82
10	1.02+3	1.23+3	1.21	1.07+3	1.05	8.36+2	0.82
20	3.96+2	5.25+2	1.32	4.30+2	1.08	3.61+2	0.91
30	1.18+2	1.43+2	1.21	1.43+2	1.21	1.25+2	1.06
40	3.65+1	-	-	4.22+1	1.16	3.98+1	1.09
50	1.17+1	1.01+1	0.86	1.28+1	1.09	1.24+1	1.06
60	3.67+0	-	-	3.69+0	1.01	3.95+0	1.08
70	1.26+0	1.07+0	0.85	1.12+0	0.89	1.32+0	1.05
80	5.88-1	3.69-1	0.63	3.23-1	0.55	4.80-1	0.82
90	2.98-1	1.70-1	0.57	9.35-2	0.31	1.98-1	0.66
100	1.63-1	1.08-1	0.66	2.72-2	0.17	9.58-2	0.59

* 3
Read as 1.48x10

(a) Values in mR/h are "the direct beam with buildup factors".
(b) Values in mR/h are "the direct beam without buildup factor" plus the single scattering component.